Robust and Economical Multi-Sample, Multi-Wavelength UV/vis Absorption and Fluorescence Detector for Biological and Chemical Contamination

Citation

Published Version

Permanent link

Terms of Use

Share Your Story

Robust and economical multi-sample, multi-wavelength UV/vis absorption and fluorescence detector for biological and chemical contamination

Peter J. Lu, Melanie M. Hoehl, James B. Macarthur, Peter A. Sims, Hongshen Ma et al.

Related Articles

Additional information on AIP Advances

Journal Homepage: http://aipadvances.aip.org

Journal Information: http://aipadvances.aip.org/about/journal

Top downloads: http://aipadvances.aip.org/most_downloaded

Information for Authors: http://aipadvances.aip.org/authors

Robust and economical multi-sample, multi-wavelength UV/vis absorption and fluorescence detector for biological and chemical contamination

Peter J. Lu (陸述義),[1] Melanie M. Hoehl,[2,3] James B. Macarthur,[1]
Peter A. Sims,[4,5] Hongshen Ma,[3,6] and Alexander H. Slocum[3]

[1]*Department of Physics and SEAS, Harvard University, Cambridge, Massachusetts 02138, USA*

[2]*Harvard-MIT Division of Health Sciences Technology, Cambridge MA 02139 USA*

[3]*Department of Mechanical Engineering, MIT, Cambridge MA 02139 USA*

[4]*Department of Biochemistry and Molecular Biophysics, Columbia University Medical Center, New York, New York, 10032, USA*

[5]*Columbia Initiative in Systems Biology, Columbia University Medical Center, New York, New York, 10032, USA*

[6]*Department of Mechanical Engineering, University of British Columbia, Vancouver, British Columbia, Canada V6T 1Z4*

We present a portable multi-channel, multi-sample UV/vis absorption and fluorescence detection device, which has no moving parts, can operate wirelessly and on batteries, interfaces with smart mobile phones or tablets, and has the sensitivity of commercial instruments costing an order of magnitude more. We use UV absorption to measure the concentration of ethylene glycol in water solutions at all levels above those deemed unsafe by the United States Food and Drug Administration; in addition we use fluorescence to measure the concentration of *d*-glucose. Both wavelengths can be used concurrently to increase measurement robustness and increase detection sensitivity. Our small robust economical device can be deployed in the absence of laboratory infrastructure, and therefore may find applications immediately following natural disasters, and in more general deployment for much broader-based testing of food, agricultural and household products to prevent outbreaks of poisoning and disease. *Copyright 2012 Author(s). This article is distributed under a Creative Commons Attribution 3.0 Unported License*. [http://dx.doi.org/10.1063/1.4738962]

I. INTRODUCTION

Commercial laboratory spectrophotometers and fluorometers are particularly useful for identifying the presence of unknown compounds, and for characterizing the absorption, emission and/or fluorescence spectra over a broad range of user-determined wavelengths, with great specificity and flexibility. However, these instruments generally require a laboratory environment: the mechanical components that enable the wide range of precisely-selectable wavelengths, including movable diffraction gratings and lens assemblies, demand mechanical and thermal stability, while the halogen lamps that generate UV wavelengths used for absorption or fluorescence require significant electrical power. As a result, these precision instruments are generally unsuitable for use outside the laboratory. There are a number of handheld devices that are starting to bridge the gap between laboratory and field analysis, but these are still typically orders of magnitude too expensive for widespread field use where they are needed to test, for example, food safety.

There are indeed many situations where the ability to measure absorption and fluorescence outside of the laboratory can be critically important; for example, detecting contaminants in food, medicine and agricultural products in the field, or evaluating microbial contamination of drinking water in the immediate aftermath of a natural disaster. In many countries, contamination testing is simply not performed, on account of the cost of analytical laboratory equipment and a scarcity

of trained users.[1–3] In many of these cases, the specific wavelengths of interest to be probed are *a priori* known, and the user would simply like to measure the absorption or emission, and / or the subsequent time evolution of these quantities, at known wavelengths. For example, detecting contamination of known compounds, or monitoring the progress of reactions involving known dyes or fluorophores, are often-used applications where the spectra are known, but the absolute measure of intensity and its time evolution are of interest. In many of these cases, particularly those involving contamination, the ability to do spectroscopy outside the laboratory environment and in the field can be of tremendous value. By fixing wavelengths, the mechanical complexity of instruments to detect absorption and fluorescence may be removed, opening up the possibility of precise measurements outside the laboratory.

In this paper, we present a new device we created in response to the many cases of DEG poisoning of children we read about because we felt as engineers we should be able to create a robust affordable detection device whose very deployment could potentially deter the substituion of DEG for gylcerine. Our device combines multiple UV/vis absorption and fluorescence detectors, in a geometry allowing simultaneous, multi-channel measurement of the time evolution of multiple samples, with single-wavelength sensitivity comparable to laboratory instruments that cost many orders of magnitude more. By combining the data from two wavelengths, substances that may have a significant background measured at one wavelength can benefit from data collected in the other, where the background signal may be substantially less. This significantly increases the signal-to-noise ratio in the measurement, and thus its effective sensitivity. To test our hypothesis, we use UV absorption to monitor the progress of a commercially-available enzyme-based kit to quantify the concentration of a major chemical contaminant, ethylene glycol (EG), in water—which in the past has episodically killed or sickened hundreds; we measure EG concentrations correctly in water, at all levels above those deemed safe by the United States Food and Drug Administration (FDA) and the European Community.[4,5] In addition, we use fluorescence to measure the concentration of glucose using a simple dye-based enzyme kit, and find that the accuracy and sensitivity of our device equals that of a commercial plate reader. Our device is completely self-contained and has no moving parts, can run on batteries or solar panels, can connect wirelessly, and can employ a mobile-phone / tablet platform for computation, data analysis and network connectivity. Consequently, our device can be deployed essentially independent of infrastructure—such as in remote or disaster-stricken areas— where laboratory instruments simply cannot be used; our technology might therefore provide key information to first-responders in preventing further tragic episodes. Moreover, the rapid measuring time and very affordable nature of our device and concomitant chemistry allow our system to be widely deployed in a practical manner, potentially enabling substantially broader systematic testing of foods, household products and medicines, the vast majority of which are simply not tested at present;[6] thus, our system may have the potential to decrease significantly the number of poisoning incidents worldwide and save lives.

II. DESIGN AND FABRICATION

Our overall design philosophy uses low-cost, commercially-available elements, precisely positioned using molded-in-place reference features with respect to a sample, to provide maximum mechanical and optical repeatability that then simplifies data analysis, while minimizing complexity and therefore the cost of manufacturing and deployment. By combining multiple UV and visible light sources and detectors in close proximity to illuminate the sample, we achieve greater detection robustness. Our design can be evolved easily to add an additional light source such as an infrared source/detector, made possible by using a cylindrical test tube, as opposed to a traditional rectangular cuvette, that is then encircled by the sensors and detectors. Simple injection-molded parts allow for the insertion of different thin plastic filters, LEDs and detectors in close proximity to each other and the test tube. To cover a wide range of wavelengths, traditional spectrophotometers and fluorometers use a broadband UV/vis light source and movable diffraction gratings, costly precision components that are mechanically fragile, and require constant maintenance and calibration. In our device, because the spectra of the substances to be detected are *a priori* known, we can choose an illumination source that emits in a narrow range of wavelengths. Lasers could be a convenient
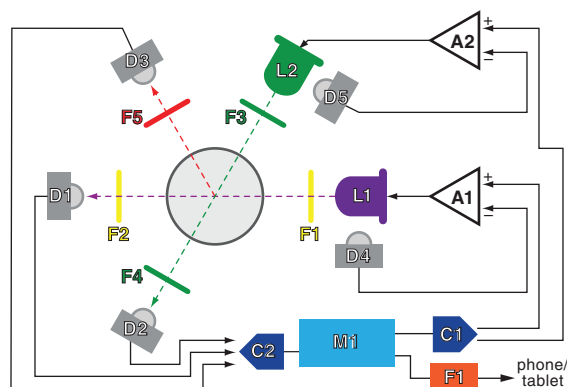
FIG. 1. Device schematic. UV light emitted by an LED (L1) passes through an excitation filter (F1), the sample, and another filter (F2) before its absorption is detected (D1). Optical feedback using an additional sensor (D4) and op-amp (A1) maintains a constant light output from L1, whose level is set by the microcontroller (M1) via a voltage generated by a D/A converter (C1). Light from a similarly stabilized green LED (L2, D5, A2) is filtered (F3) before passing through the sample; green light is filtered and detected for green absorption (F4, D2) and red fluorescence (F5, D3). Voltage outputs from the detectors (D1, D2, D3) are digitized by an A/D converter (C2) and sent to the microcontroller (M1), which formats and transmits the data via USB (F1) to a computer, smart mobile-phone or tablet.

choice, but LEDs are generally more rugged and compact, require less power, and are now available in a wide variety of wavelengths from the deep UV to long-wavelength IR. Furthermore, they can be extremely inexpensive, costing a few cents to dollars, orders of magnitude less than the xenon lamp in a typical spectrophotometer. We choose a standard LED size for illumination, which allows us to take advantage of the wide variety of wavelengths available commercially—and any LED in the same form factor can be substituted without modification to either the device electronics or mechanical structure.

The spectra of some LEDs, though centered around a desired wavelength, can have relatively broad tails. To improve the spectral specificity of these LEDs for spectroscopy, we filter out undesired wavelengths with body-colored polycarbonate films (Roscolux) designed for theatrical lighting, which are very inexpensive and designed for durability in high-heat and light environments; the small pieces we use in our device cost fractions of a cent.

The general geometry for absorption detection is shown in the device schematic in Fig. 1. To measure absorption, we illuminate the liquid sample with an LED (L1) and measure the intensity change after the light has passed through the sample, using a photodiode. For simplicity and robustness, we choose a form of photodiode integrated with an op-amp in a single package (D1), which outputs a voltage proportional to the incident light striking the photodiode (Texas Advanced Optoelectronic Solutions TSL257); this semiconductor light-to-voltage detector costs around a dollar. The low cost of this detector component allows us not only to use it for the primary absorption measurement, but also to include a second detector (D4) next to the LED; we couple it to an active feedback loop with an op-amp (A1) to stabilize the LED's intensity at a constant level even as temperature changes, due to the external environment or as the LED is powered on. The circuit is a single-amplifier proportional servo with a bandwidth of 1 KHz, which effectively removes thermal drift and reduces errors from mechanical vibration. The high-level voltage output of the sensor makes for a simplified servo circuit—each LED's driver adjusts the LED current until the sensor voltage equals the voltage set by the microcontroller (M1) via a D/A converter (C1). This active illumination stabilization, a feature found in advanced laser systems, is crucial to reproducible light intensity measurements. The analog voltage from the detector is converted via an A/D converter (C2) to a digital value that is sent to a microcontroller (M1), then as ASCII over wired or wireless USB (U1) to a Linux-based (Ubuntu) host, where the data processing and analysis (C++), storage and communication are performed. The output data is a simple list of 16-bit integers, corresponding to the digitized voltage levels from each light-to-voltage detector; 16 bits are sufficient to capture all of the signal above the noise from the detectors, but we use 24-bit detectors because present discrete
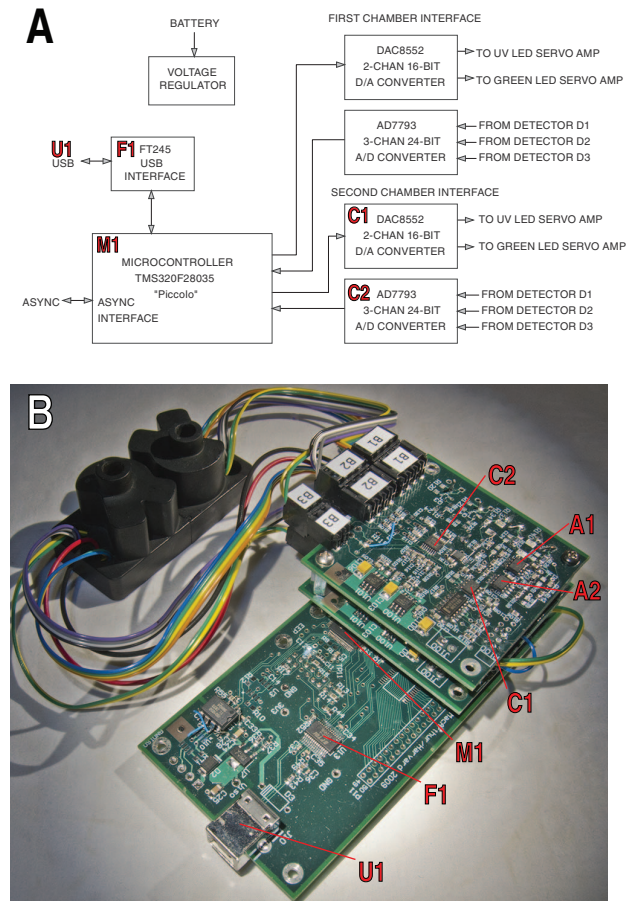
FIG. 2. (A) Circuit diagram showing specific electrical components of our detector, with microcontroller (M1), D/A converter (C1), A/D converter (C2) and USB Interface (F1) components labeled as in Fig. 1. (B) Photograph of the detector (black, upper left) and circuit boards, with major components labeled with red letter corresponding to labels in (A) and in Fig. 1.

inexpensive A/D converters all use this higher resolution. We use a variety of host computing platforms, including an ordinary Intel-based laptop, and an ARM-based mobile phone / tablet platform (NVIDIA Tegra family), with equivalent functionality. A circuit diagram with specific components is shown in Fig. 2(A); a photograph of the circuit boards and the device itself is shown in Fig. 2(B).

The LED, sample, detector and filters are held in place deterministically by an opaque plastic enclosure that is extremely simple to manufacture and robust in use. The actual device appears in the photograph in Fig. 2(B). A 3D model of the device, raytraced on an NVIDIA Tesla C2050 GPU using Bunkspeed Pro, with one of the two enclosures removed to show the position of the LEDs and detectors, is shown in Fig. 3(A). This monolithic structure is designed for two-part mold injection molding with no side pulls; our experimental unit is made by stereolithography (SLA), and in production would cost less than a dollar. We achieve high-precision location of the LED, sample, and detectors by using the components' leads themselves as flexure spring features, which force the components against reference features, all within the same monolithic part. The bottom of the enclosure is shown in Fig. 3(B), showing a clear view of the cavities to hold the components; a close-up of one of the light-to-voltage detector cavities in shown in Fig. 3(C). A key to successful optical detection is to create a very thin slit to receive the plastic filter without allowing any light leakage. To mold such a slit using a thin core would not be practical, so instead larger near-overlapping mold cores are used, such that when the mold is opened, an effective thin gap is created, as shown in Fig. 3(C).
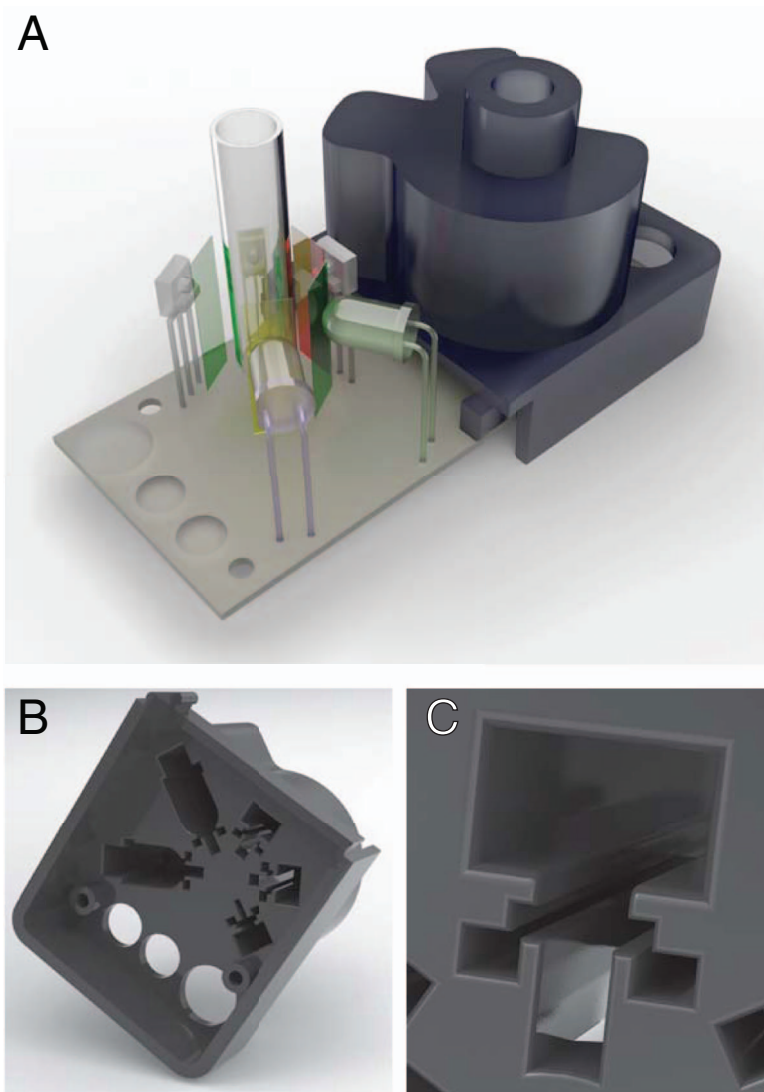
FIG. 3. (A) 3D model of our as-built device. One chamber has the black plastic enclosure removed, to illustrate the positions of LEDs, filters and sample-holding test tube. (B) View of the bottom of the plastic enclosure, showing openings for two LEDs (L1 and L2 in Fig. 1) and 3 light-to-voltage detectors (D1, D2 and D3 on Fig. 1). (C) Close-up of the opening for one light-to-voltage detector, showing slit for thin filter plastic.

To enable the sample to be illuminated from multiple sources in a small space, we use a round glass test tube (Durham 6×50 culture tube) as our chemical reaction chamber, whose hemispherical bottom rests in a hemispherical seat to establish axial and radial position; clearance around the test tube walls accommodates tolerances, while use of a test tube with length-to-diameter ratio greater than ten keeps the tilt of the test tube to a level that does not affect the readings. Our mechanically-robust design has no moving parts and ensures positional repeatability; samples removed, reinserted, or measured in a different test tubes, all yield the same results.

III. PRELIMINARY EXPERIMENTS AND RESULTS

We conduct an initial series of tests to validate the design and enable us to plan for further measurements. We first test the UV absorption capabilities of our device with an enzyme-based assay that detects the presence of ethylene glycol (EG), an important component of automotive
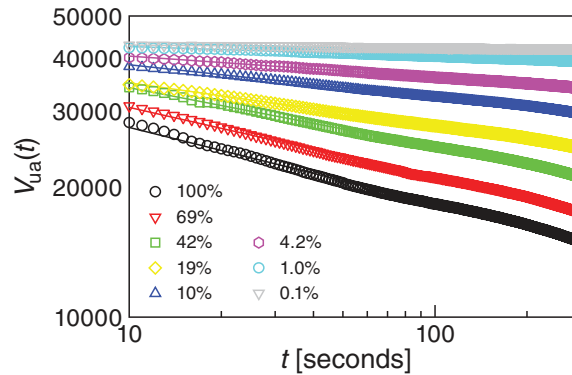
FIG. 4. Time evolution of output voltage $V_{ua}(t)$ from the UV detectors, digitized as 16-bit integer, shown on a log-log plot with symbols for different EG concentrations c_ϵ in water. The data fall onto a straight line for each sample, demonstrating power-law scaling. The magnitude of the slope of each line $\gamma(c_\epsilon)$ varies monotonically with c_ϵ.

antifreeze that is sometimes improperly substituted for propylene glycol and polyethylene glycol in medicines, household products and foods, with lethal consequences.[7] Within the human body, EG is first digested by alcohol dehydrogenase (ADH) into an aldehyde, then into various acids, which are the direct cause of physiological damage.[1] To detect EG, we choose an ADH-based enzyme assay, which converts a hydroxyl group to an aldehyde, and at the same time converts the coenzyme NAD^+ into NADH.[8] NADH has a broad absorption peak from 350-370 nm, so that the measured absorption of UV light in that wavelength range should reflect the amount of EG; we therefore select a UV LED (ledsupply.com L5-0-U5TH15-1) with a peak emission of $\lambda = 365$ nm, to illuminate the sample.

To measure c_ϵ, the mass fraction (concentration) of EG, we add a solution of ADH to the sample, immediately insert into the sample chamber, and record the voltage $V_{ua}(t, c_\epsilon)$ measured by the UV absorption detector once per second for five minutes. For pure EG ($c_\epsilon = 1$), the $V_{ua}(t, c_\epsilon)$ data fall on a straight line when plotted on a log-log plot, demonstrating a power-law behavior, as shown by the black circles in Fig. 4. Because our test tube has a circular cross section and the LED has a distribution of illumination angles, a single path-length is not well-defined; therefore, we cannot rely on a simple Beer's Law calculation for the absolute absorbance, particularly as there may be slight lensing effects. Instead, we measure samples of known c_ϵ in water, from the FDA safety limit of $c_\epsilon = 10^{-3}$ to $c_\epsilon = 1$.[4] This allows us to establish a calibration curve, accounting for the slight variations in position and brightness / sensitivity of the electronic components that will naturally vary from detector to detector. In all cases we observe lines on the log-log plot; $V_{ua}(t, c_\epsilon) \propto t^{-\gamma(c_\epsilon)}$, as shown with colored symbols in Fig. 4.

The power-law exponent magnitudes $\gamma(c_\epsilon)$ monotonically increase with c_ϵ, as shown with the blue circles in Fig. 5. The optical feedback loop stabilization (L1, D4 and A1 in Fig. 1) ensures that LED intensity remains constant irrespective of environmental changes; thus, there are no adjustable parameters in our determination of $\gamma(c_\epsilon)$. These data demonstrate our ability to measure c_ϵ in drinking water, which has caused sickness and death even in the United States,[9] at all concentrations deemed unsafe by the FDA. To confirm the absolute, not just relative, accuracy of our data, we also measure antifreeze samples with known EG concentrations, following the same chemical protocol. Strikingly, we find that these samples fall on the same curve as the EG in water, shown by the green squares in Fig. 5. These data demonstrate that our measurements may provide a quantitatively accurate way to measure absolute EG concentration.

In addition to absorption, fluorescence is another common spectroscopic technique. The use of different filters allows us to excite at one wavelength, and detect emission at a longer one. The circular geometry of the system, with the light-tight filter-holding features, allows us to integrate a second, separate fluorescence channel for the same sample as the absorption detection channel without any interference. Hence we add another LED spaced 60° from the UV LED for excitation, and two additional light detectors, using differently-colored theater gel plastic to filter the green
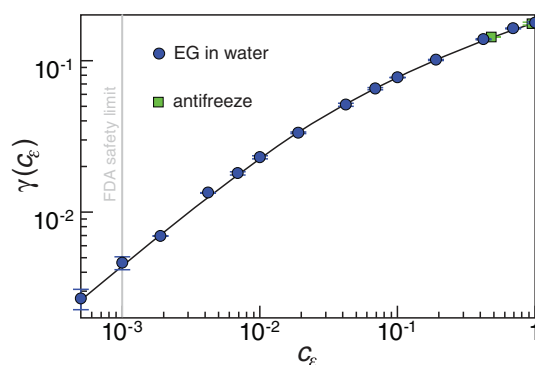
FIG. 5. $\gamma(c_\epsilon)$ varies monotonically with c_ϵ, shown with blue circles for pure EG in water, and green squares for antifreeze, which follow the same trend, shown in black as a guide to the eye. Data point represent averages over several runs, with error bars corresponding to the standard deviation of the measurements. FDA safety limit $c_\epsilon = 10^{-3}$ is indicated with a grey vertical line.

absorption and red fluorescence, placed at 180° and 60°, respectively, relative to the green LED. We choose these angles to accomodate all of the LEDs and detectors, as using 90° square geometry does not allow enough detectors to capture both UV absorption and visible fluorescence simultaneously. The complete illumination and detection scheme is shown in Fig. 1. We choose a green LED (Cree LC503FPG1-15P-A3) with a peak emission of $\lambda = 527$ nm for illumination in this fluorescence channel, as there are a number of common red dyes that are excited by light in this range; however, as in the case of the UV LED, any color can be substituted within the same housing with the same electronics.

By offsetting the activation of the UV and green LEDs by 0.5 seconds, we collect data from both UV-illuminated and green-illuminated channels once each second, with no possible crosstalk. Thus, our device simultaneously measures absorption and fluorescence with two excitation wavelengths and has no moving parts—which is not possible with the square cuvette geometry traditionally found in laboratory fluorometers and spectrophotometers. Moreover, the low cost of our detector and electronics makes it economical for us to construct a second, identical, multi-channel detector. This provides the capability to run control reactions in parallel, so that the absolute activity of particular enzyme samples can be divided out; the two-chamber final device is shown in Figs. 2(B) and 3(A).

To test the capability of our fluorescence detector, we measure the concentration of glucose with a commercial kit based on the activity of glucose oxidase (Invitrogen Amplex Red Glucose / Glucose Oxidase Assay Kit A22189). In this assay, glucose oxidase reacts with *d*-glucose to form *d*-gluconolactone and H_2O_2. In the presence of horseradish peroxidase (HRP), the H_2O_2 reacts with the Amplex Red reagent in a 1:1 stoichiometry to generate a red fluorescent oxidation product, related to resorufin, which emits a bright red color when excited with green light. We prepare the various enzyme and dye solutions following the manufacturer's protocol, and run the reaction on samples of various concentrations of *d*-glucose, ranging from 0.4 μM to 400 μM. The UV absorption and green fluorescence values are monitored in the detector for 5 minutes and again measured after 30 minutes to provide a stationary fluorescence value after the reaction is complete. At the same time as each sample is run, we also run a second control sample with a *d*-glucose concentration of 200 μM in the second chamber, whose value we divide out in order to cancel the effects of variations with enzyme activity. This normalization, made possible by the presence of the second detector, allows us to quantify the amount of *d*-glucose at all concentrations greater than few μM, as shown in Fig. 6.

We compare the sensitivity of our device to that available in commercial instruments, running the same set of samples with the same enzyme kit in a fluorescence plate reader (Molecular Devices, SPECTRAmaxTM GEMINI XS), exciting at 530 nm, and detecting at 590 nm, again after 30 minutes. Our device has the same lower-limit of detectable *d*-glucose concentrations as the commercial plate reader, which costs several orders of magnitude more, as shown in Fig. 6.
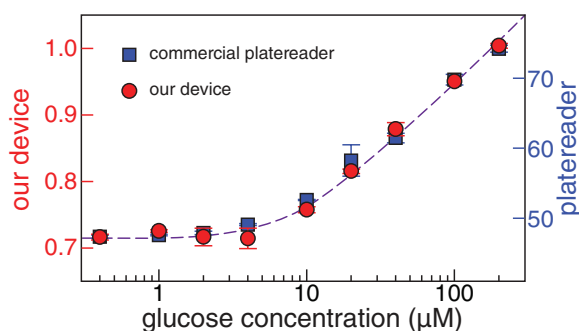
FIG. 6. Comparison of the detection of the same glucose oxidase-based reaction, which generates a fluorescent product, in our detector and in a commercial fluorscence plate reader. Data point represent averages over several runs, with error bars corresponding to the standard deviation of the measurements.

IV. CONCLUSIONS AND FURTHER WORK

The capabilities of our device make it suitable for a broad range of applications where spectroscopic wavelengths are *a priori* known. The individual channels within our detector have sensitivity comparable to commercial laboratory instruments costing orders of magnitude more; moreover, the low cost of our device makes practical the multiple channels and samples that allow us to normalize by references and combine data from different simultaneous measurements to remove background and substantially increase the signal-to-noise ratio. Our device is self-contained, in contrast to the array of pumps and additional off-chip infrastructure needed to support a microfluidic device. It consumes sufficiently low power to run on batteries or a solar panel, is mechanically rugged and functions in the absence of external infrastructure; hence our device has potential application in remote areas and disaster situations where even the most basic measurements have the potential to save many lives.

Widespread deployment of the device we have presented, or variants thereof, coupled with the network connectivity and geo-location technology present in the smart mobile-phone / tablet platform we use for analysis and computation, can facilitate automated aggregation of data remotely; we can imagine that geographic and temporal patterns, for example, in detected contamination may allow earlier identification of outbreaks than is now possible, adding a new tool to control and lessen the effects of epidemics. Finally, the fast detection of our assays—only a few minutes—allows rapid testing of perishable foods and ingestible products which are not tested because current culturing-based methods require days; this new capability may have potential applications in much broader sampling of both domestic and imported foods and agricultural products, enabling for the first time end-to-end characterization within a food or medicine supply chain.

[1] R. Gomes, R. Liteplo, and M. E. Meek, *Ethylene glycol: human health aspects* (World Health Organization, 2002).
[2] V. Velusamy, K. Arshak, O. Korostynska, K. Oliwa, and C. Adley, Biotech. Adv. **28**, 232 (2010).
[3] P. Yager, G. J. Domingo, and J. Gerdes, Annu. Rev. Biomed. Eng. **10**, 107 (2008).
[4] United States Food and Drug Administration, *Guidance for Industry: Testing of Glycerin for Diethylene Glycol* (2010).
[5] European Commission Scientific Committee on Consumer Products, *Opinion on Diethylene Glycol* (2008).
[6] United States House of Representatives Subcommittee on Science and Technology, *FDA: Science and Mission at Risk* (2007).
[7] EG poisonings episodically kill hundreds in third-world countries, even today. The realization that there is no existing low-cost method for detecting such poisons motivated the research that led to the device and chemistry methods presented here.
[8] J. H. Eckfeldt and R. T. Light, Clin. Chem. **26**, 1278 (1980).
[9] S. Schultz *et al.*, Morb. Mortal. Wkly. Rep. **36**, 611 (1987).